journal

J. Am. Ceram. Soc., 78 [1] 137–45 (1995)

The Evolutionary Process during Pyrolytic Transformation of Poly(N-methylsilazane) from a Preceramic Polymer into an Amorphous Silicon Nitride/Carbon Composite

Richard M. Laine,*,†,‡,§ Florence Babonneau,¶ Kay Y. Blowhowiak,§ Richard A. Kennish,§ Jeffrey A. Rahn,‡,†† Gregory J. Exarhos,*,‡‡ and Kurt Waldner‡

Department of Materials Science and Engineering, University of Michigan, Ann Arbor, Michigan 48109-2136

Department of Materials Science and Engineering, University of Washington, Seattle, Washington 98195

Laboratoire de la Matiere Condensee, Universite Pierre et Marie Curie, Paris, France

Department of Chemistry, Eastern Washington State University, Cheny, Washington 99004

Battelle Pacific Northwest Laboratories, Richland, Washington 99352

The pyrolytic evolution of poly(N-methylsilazane), $-[H_2SiNMe]_x-$, from preceramic polymer to ceramic product is followed by heating samples of the partially cross-linked polymer, in 200°C increments, from ambient temperature to 1400°C. The intermediate products are characterized by chemical analysis, diffuse reflectance Fourier transform IR spectroscopy (DRIFTS), Raman spectroscopy, and ^{29}Si and ^{13}C magic-angle spinning (MAS) solid-state NMR. Spectroscopic characterization indicates that the 1400°C pyrolysis products are amorphous silicon nitride mixed with amorphous and graphitic carbon (as determined by Raman spectroscopy), rather than silicon carbide nitride, as expected based on the presence of up to 20 mol% retained carbon. Efforts to crystallize the silicon nitride through heat treatments up to 1400°C do not lead to any crystalline phases, as established by transmission electron microscopy (TEM) and small-area electron diffraction (SAD). It appears that the presence of free carbon, along with the absence of oxygen, strongly inhibits crystallization of amorphous silicon nitride. These results contrast with the isostructural poly(Si-methylsilazane), $-[MeHSiNH]_x-$, which is reported to form silicon carbide nitride on pyrolysis.

I. Introduction

Efforts in these and other laboratories to develop easily processable silicon nitride polymer precursors have focused primarily on Si-substituted polysilazanes ($-[RHSiNH]_x-$, R = H, alkyl, or aryl) and silsesquiazanes, $-[RSiN_{1.5}]_x-$, with most of the work centered on poly(Si-methylsilazane), $-[MeHSiNH]_x-$, and the related silsesquiazanes, $-[MeSi(NR)_{1.5}]_x-$.[1–13] In all instances, pyrolysis of poly(Si-Rsilazane)s to temperatures of 1000°–1300°C in N_2 leads to atomically disordered materials (by NMR and XRD) that exhibit, at best, only limited crystallinity. In particular, pyrolysis of various related poly(Si-methylsilazane)s gives ceramic products that contain ≈5–20 mol% carbon.

Physicochemical characterization of these materials indicates that they are not amorphous mixtures of silicon nitride, carbon, and silicon carbide, but rather silicon carbide nitride wherein the average silicon has three bonds to nitrogen and one to carbon. We describe here the pyrolysis of poly(N-methylsilazane), $-[H_2SiNMe]_x-$; which in contrast to $-[MeHSiNH]_x-$, results in the formation of a composite ceramic product containing what appears to be phase pure Si_3N_4 and significant quantities of C, rather than silicon carbide nitride.

As part of our continuing interest in preceramic polymers, we have synthesized polysilazane precursor $-[H_2SiNMe]_x- \equiv MeNH[H_2SiNMe]_x-[HSi(NMe)_{1.5}]_y-H$; poly(N-methylsilazane), according to the following chemical reactions:[10–13]

$$H_2SiCl_2 + 3MeNH_2 \xrightarrow{Et_2O/-78°C} 2MeNH_3Cl + MeNH[H_2SiNMe]_x-H \quad (M_n \approx 1200\ Da) \quad (1)$$

$$MeNH[H_2SiNMe]_x-H \xrightarrow{Ru_3(CO)_{12}/65°C/40–60h} MeNH[H_2SiNMe]_x-[HSi(NMe)_{1.5}]_y-H + H_2 \quad (M_n \approx 2000\ Da) \quad (2)$$

Poly(N-methylsilazane), $-[H_2SiNMe]_x-$, is isostructural with and chemically identical to (on a monomer basis) $-[MeHSiNH]_x-$. Thus, studies on the pyrolytic transformation of $-[H_2SiNMe]_x-$ to ceramic product represent an excellent test of the influence of changes in polymer architecture on selectivity to ceramic products and control of the resulting microstructure.

We previously reported[10,12] that pyrolysis of $-[H_2SiNMe]_x-$ ($M_n \approx 2300$ Da, 5°C/min/N_2 to 1000°C, 2-h hold, 63% ceramic yield) leads to a material with a composition of $Si_{1.66}C_{1.5}N_{2.4}H_{1.11}O_{0.06}$. This composition was interpreted to indicate an apparent ceramic composition of 77% Si_3N_4, 18% excess C and 3% excess N. This interpretation was based on a simple accounting method wherein it was assumed that all of the Si reacts with as much nitrogen as possible to form Si_3N_4. Any Si not accounted for by combination with N is then combined with C to form SiC. The remaining carbon and/or nitrogen is assumed to be retained in non-silicon-containing species. No effort was made to consider thermodynamics in this accounting system, nor was the presence of hydrogen considered. This approach was used simply for comparison with the results obtained in related studies on the pyrolysis of $-[MeHSiNH]_x-$.

Z. A. Munir—contributing editor

Manuscript No. 193747. Received September 2, 1993; approved June 19, 1994.

Supported by the Office of Naval Research through Contract Nos. N00014-88-K-0305 and N00014-92-J-1711. RML was partially supported by the IBM Corporation and the Army Advanced Materials and Technology Laboratory. Travel for RML and FB supported by NSF/CNRS Travel Grant No. INT-9216604.

*Member, American Ceramic Society.

†Author to whom correspondence is to be addressed.

‡University of Michigan.

§University of Washington.

¶Université Pierre et Marie Curie.

††Eastern Washington State University.

‡‡Battelle Pacific Northwest Laboratories.

An insoluble $-[MeHSiNH]_x-$ polymer, from reactions (3) and (4), was also pyrolyzed under identical conditions to give an identical ceramic yield (63% at 1000°C) and a chemical

$$MeHSiCl_2 + 3NH_3 \xrightarrow{Et_2O/-78°C} 2NH_4Cl + NH_2[MeHSiNH]_x-H \quad M_n \approx 1100\ Da \quad (3)$$

$$NH_2[MeHSiNH]_x-H \xrightarrow{Ru_3(CO)_{12}/65°C/40\text{–}60\ h} NH_2[MeHSiNH]_x-[MeSi(N)_{1.5}]_y-H + H_2 \quad (4)$$

composition of $Si_{1.99}C_{1.38}N_{1.68}H_{0.54}$. Using the same accounting technique, the apparent ceramic composition is 64% Si_3N_4, 25% SiC, and 9% excess C. Soluble analogs give similar compositions but with lower ceramic yields.[11–13]

If we rely on the apparent ceramic compositions calculated for the Si–Me and N–Me polysilazane derived ceramic materials to establish selectivity to ceramic product, then it appears that the changes in monomer architecture result in a significant difference in selectivity to ceramic products.[14] Unfortunately, the accounting method, for the reasons mentioned above, provides only a qualitative indication of the differences in product selectivity.

As will be detailed at a later date, the ceramic material produced by pyrolysis of $-[MeHSiNH]_x-$ is a mixture of silicon carbide nitride and excess carbon.[14,15] ^{29}Si MAS-NMR spectra of these and related materials show extreme diversity in the magnetic environment at Si as a result of species wherein Si is bound to four carbons (SiC_4), three carbons and one nitrogen (SiC_3N), etc.[16–20] Thus, the apparent ceramic composition reported previously does not describe the true nature of these precursor-derived materials. One obvious question is whether the same problem exists with the poly(N-methylsilazane) derived materials.

We have now examined, by chemical analysis, Raman spectroscopy, MAS solid-state NMR, and DRIFTS, the events that occur as $-[H_2SiNMe]_x-$ slowly transforms from polymer to ceramic during pyrolysis from ambient temperature to 1400°C. We find that in contrast to the poly(Si-methylsilazane) results, the primary ceramic phases produced are actually consistent with the apparent ceramic composition. The silicon nitride-containing products described here are similar to amorphous materials formed in the Tonen "silicon nitride" fibers and those produced by ammonolysis of silicon carbide nitride.[21–25]

II. Experimental Procedure

(1) General Procedures

All operations were carried out with the careful exclusion of extraneous air and moisture. Air- and moisture-sensitive materials were manipulated using standard Schlenk and glove-box techniques. All chemicals were purchased from standard vendors. Ether was distilled from sodium benzophenone ketyl under nitrogen before use.

(2) Polymer Synthesis

Poly(N-methylsilazane) was prepared by reacting H_2SiCl_2 with excess $MeNH_2$ in ether at -78°C and was partially cross-linked, after removing solvent, by heating to 65°C with ≈0.2 mol% $Ru_3(CO)_{12}$ as catalyst, according to published procedures.[10–15] Poly(Si-methylsilazane) was synthesized by reacting $MeHSiCl_2$ with excess NH_3 in ether at -78°C and was partially cross-lined using identical procedures.[10–15]

(3) Polymer Pyrolysis Protocols

1–2-g samples of polymer were placed in stainless steel or quartz boats in the glove box. The boats were then placed in a quartz tube that was then sealed with a quartz cap containing gas inlet and outlet ports that could be sealed against exposure to air. The sealed quartz container was then brought out of the glove box and placed in a mullite process tube (4.3-cm ID) in a Lindberg 5814 series, single-zone, horizontal tube furnace, equipped with a Eurotherm 818S programmable temperature controller. N_2 gas was purged through the pyrolysis tube as the sample was ramped to temperature at 5°C/min, held isothermally for 1 h, and then furnace cooled. Samples pyrolyzed to 1000°C were transferred from the stainless steel or quartz boat to a graphite or alumina boat for pyrolysis studies to 1400°C.

(4) Analytical Methods

(A) Chemical Analyses

Elemental analyses were performed by Galbraith Laboratories, Knoxville, TN, and at The University of Michigan, Department of Chemistry, analytical services for analysis of carbon, hydrogen, and nitrogen content (CHN). At the University of Michigan, a Perkin-Elmer (Norwalk, CT) 2400 CHN Elemental Analyzer was operated at 1075°C, with He as a carrier gas. Duplicate powder specimens (1.5 mg) were loaded into tin capsules with powdered tin (6–10 mg) as a combustion aid. Acetanilide was used as a reference standard and was analyzed in the same manner as the samples. Similar methods were used at Galbraith except that Si was analyzed by a gravimetric method. The analyses reported below are averages of two separate samples.

(B) NMR Studies

All solution spectra were run in $CDCl_3$ unless otherwise noted and recorded on a Varian 300-MHz instrument (Palo Alto, CA). Proton NMR spectra were obtained with the spectrometer operating at 300 MHz and using a 4000-Hz spectral width, a relaxation delay of 1 s, a pulse width of 82°, and 16k data points. $^{13}C\{^1H\}$ NMR spectra were obtained with the spectrometer operating at 75 Hz and using a 16000-Hz spectral width, a relaxation delay of 0.5 s, a pulse width of 60°, and 16k data points. $^{29}Si\{^1H\}$ NMR spectra were obtained on a Brüker MSL400 spectrometer (Wissembourg, France) operating at 79.5 MHz and using a 12000-Hz spectral width, a relaxation delay of 15 s, a pulse width of 5 μs, and 8k data points.

Solid-state magic-angle spinning (MAS) NMR spectra were recorded on a Brüker MSL400 spectrometer at 79.5 and 100.6 MHz for ^{13}C and ^{29}Si, respectively. The spinning rate was 4 kHz. For the ^{29}Si MAS experiments,[26–28] pulse widths of 2.5 μs ($\theta \approx 35°$) were used with delays between pulses of 60 s. For CP MAS experiments, contact times of 2 ms were used for ^{29}Si and 1 ms for ^{13}C. Sample sizes for solid-state spectra were ≈500 mg.

NMR spectra were simulated using least-squares methods. Peak parameters (chemical shift, intensity, line width, and line shape (adjusted with a Gaussian/Lorentzian ratio) were optimized to fit the experimental data. Peak integration can be estimated with an accuracy of ±3%.[27,28]

(C) Diffuse Reflectance Infrared Fourier Transform (DRIFT)

DRIFT spectra were obtained on a Mattson Galaxy Series 3020 bench adapted with a Harrick Scientific Corporation "Praying Mantis" diffuse reflectance accessory (DRA-2CO). Potassium bromide (KBr, FTIR grade, Aldrich) powder, dried under dynamic vacuum for >8 h at 110°C, was used as the nonabsorbing medium. Powder specimens were prepared by grinding analyte in an alumina mortar and pestle, weighing 0.5 wt% analyte to KBr (3 mg analyte in 650 mg KBr). The powder mixture was mixed in a polystyrene container (Crescent No. 3111) with a polystyrene ball (No. 3112) in a Wig-L-Bug Amalgamator (Crescent No. 3110-3A) for 5 min. Parameters were optimized on the bench to obtain a >5000:1 signal-to-noise ratio, and an intensity of ≈1 Kubelka–Munk unit. Typical scan conditions were 512 scans at 2 wave number resolution measured in the forward direction, with a forward mirror velocity of 0.10 cm/s (3175 Hz) and a reverse mirror velocity of 0.32 cm/s (10000 Hz). Survey scans were taken by accumulating 16 scans at 4 wave number resolution in the forward direction, with the same mirror velocities.

(D) Raman Spectra

Raman spectra were collected using either a Spex 1403 0.85-m double spectrometer equipped with a red-sensitive photomultiplier tube or a Spex Model 1877 triplemate monochromator equipped with a nitrogen-cooled CCD detector (Princeton Instruments). Powders or small lumps of the heat-treated material were excited in a backscattering geometry, and spectra were acquired using several probe wavelengths (457.9, 488.0, 632.8, and 650.0 nm) at power levels between 5 and 25 mW. Slit widths were maintained at 250 μm. Spectra were acquired using a 2-s integration time (photomultiplier detection) or a 500-s integration time (CCD).

(5) TEM Studies

(A) Sample Preparation

TEM samples were prepared by powder dispersion on a holey carbon-coated 100 mesh copper TEM grid. The sample was ground in an ultrasonically cleaned alumina mortar and pestle. The mortar and pestle were wiped clean and more sample was ground for 2–3 min to avoid alumina contamination. Powder was dispersed on the grid, and the grid was tapped to remove excess powder and placed in the double-tilt TEM sample holder such that the particles would be on the top of the grid, allowing both scanning and scanning transmission electron microscopy (SEM and STEM) imaging. Efforts to prepare samples by microtoming polymer-impregnated powders with sapphire and diamond blades were not successful, owing to the extremely hard nature of the ceramic powder product.

(a) TEM: TEM was done on a JEOL 2000FX analytical electron microscope with X-ray energy-dispersive spectroscopy (XEDS). Standard start-up and alignment procedures were followed to ensure maximum beam throughput. Beam current was between 114 and 116 μA, with an operating voltage of 200 kV.

(b) TEM Imaging and Diffraction: After identifying a particle or group of particles as being alumina-free (from grinding) and thin enough to allow good beam throughput, micrographs were taken and the location of the particle noted. Diffraction patterns were generated using the smallest available aperture to avoid contributions from neighboring particles. Diffraction patterns were also taken of the background, the carbon coating, by rolling away from any particles. Multiple particles were examined from various areas on the grid.

III. Results

(1) Chemical Analysis

The chemical analyses for the polymer pyrolyzed at selected temperatures are presented in Table I. The results of these analyses in terms of the molar ratios of the elements are plotted in Fig. 1 (to 1000°C). From room temperature to 400°C, the chemical composition of the samples is almost constant, suggesting that under the pyrolysis conditions used in these studies, the polymer is stable (i.e., does not undergo mineralization). Between 400° and 800°C, but especially between 400° and 600°C, the H content drops precipitously, suggesting that the polymer undergoes significant chemical reorganization as it decomposes to form a ceramic-like material. Thus, longer hold times at lower temperatures (e.g., 10 h at 500°C) are likely to have the same effect.

As seen in Table I and Fig. 1, the H/Si molar ratio varies from ≈5 at 400°C to ≈0.16 at 1400°C. At the same time, the N/Si ratio increases from ≈1.1 to ≈1.5 (at 800°C) before decreasing to ≈1.28 at 1400°C, while the C/Si ratio decreases from ≈1.3 to ≈0.86 at 1400°C. The compositional changes are more pronounced as the polymer transforms to ceramic in the 400°–600°C range. Above 600°, the compositions change, but in a more subtle manner. The C/Si ratio varies slightly, ranging between 0.93 at 800°C and 0.86 at 1400°C (from Table I); coincidentally, the hydrogen content drops to <0.3%. The N/Si ratio drops from a 1.5 maximum at 800°C to 1.28 (from Table I) as the sample is heated to 1400°C. At this point, the N/Si ratio is slightly less than the 1.33 expected for pure silicon nitride.

Table I. Elemental Composition (Molar Amounts) of the Intermediates Formed by Pyrolysis of Poly(N-methylsilazane) to Selected Temperatures*

Pyrolysis temperature	Composition			
	C	H	N	Si
RT	1.12	4.98	1.12	1.0
200	1.68	7.84	1.62	1.50
400	1.76	6.86	1.54	1.36
600	1.44	2.39	2.28	1.65
800	1.51	0.93	2.54	1.63
1000	1.50	0.70	2.40	1.66
1400	1.52	0.28	2.27	1.76

*Polymer $M_n \approx 2300$ D with a ceramic yield of 63% at 900°C.[10,12] Polymer heated at a ramp rate of 5°C/min/N_2 followed by a 1-h hold at temperature.

(2) NMR Results

The liquid-phase ^{29}Si NMR spectrum shown in Fig. 2 is that obtained from a bulk sample (1 g) of $-[H_2SiNMe]_x-$ heated to 200°C and then dissolved in $CDCl_3$. It is dominated by a triplet characteristic of $[H_2\underline{Si}NMe]_x$ sites ($\delta = -24.7$ ppm; $|J_{Si\text{-}H}| =$ 222 Hz).[30] The peaks between −37 and −47 ppm likely arise as a consequence of two kinds of chain termini $H_3\underline{Si}NMe$ ($\delta_1 = -41.3$ ppm; $|J_{1Si\text{-}H}| = 208$ Hz, and $CH_3NH\underline{Si}H_2$($\delta_2 = -43.5$ ppm; $|J_{2Si\text{-}H}| = 207$ Hz)). These sites represent 7% of the total Si sites. The presence of other peaks between −25 and −30 ppm arises from cross-linked Si, e.g., $-[H\underline{Si}(NMe)_{1.5}]-$ and $-[\underline{Si}(NMe)_2]-$. However, the sharp peaks observed indicate that the types of Si magnetic environments in the polysilazane are well defined and therefore relatively few in number.

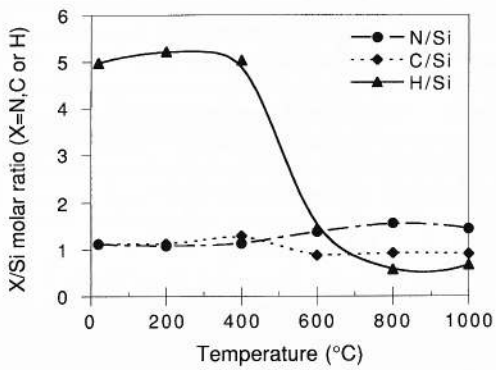

Fig. 1. Molar ratios for poly(N-methylsilazane) heated to selected temperatures. Polymer $M_n \approx 2300$ D with a ceramic yield of 63% at 900°C.[10,12]

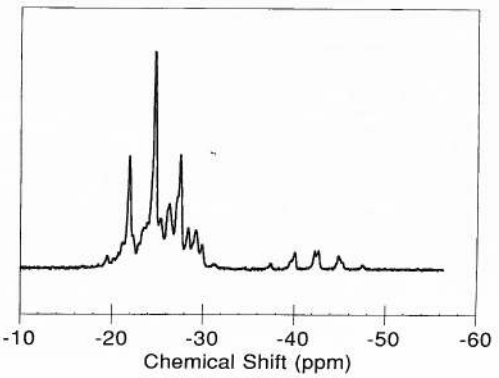

Fig. 2. ^{29}Si NMR solution spectrum ($CDCl_3$) of $-[H_2SiNMe]_x-$ heated to 200°C for 1 h in N_2.

The corresponding ^{13}C NMR solution spectrum for the 200°C polymer shows the presence of three types of N-$\underline{C}H_3$ at 27.9, 29.6, and 31.1 ppm. The ^{29}Si MAS NMR spectra of 1-g samples heated in 200°C increments (5°C/min/N_2/1-h hold) from 200° to 1000°C are shown in Fig. 3(a).

(A) 400°C

At this temperature, the well-defined peaks of the 200°C polymer do not shift, but broaden considerably as is typical of a highly cross-linked polymer. Cross-linking immobilizes the polymer chains, which in turn broadens the distribution of magnetic environments about the various Si centers, especially the chain ends. This is in keeping with the chemical analyses which support the continued existence of a polymeric material.

A cross-polarized (CP) ^{29}Si MAS NMR (Fig. 3(b)) was also run on the 400°C sample. CP techniques provide better signal-to-noise ratios as long as there are hydrogens near the Si centers. In addition, proton decoupling during signal acquisition allows better resolution of the various Si centers. At 400°C, two peaks at −18 and −30 ppm show much enhanced intensities, especially the −18-ppm peak, as a consequence of cross-polarization. As discussed below, these peaks are attributed respectively to silicon centers of the type SiH_2N_2 (e.g., $-H_2SiNMe-$) and $SiHN_3$ [$HSi(NMe)_{1.5}$].

The corresponding ^{13}C CP MAS NMR spectrum shown in Fig. 4 gives a single, rather sharp peak (560-Hz linewidth) centered at 28.5 ppm, indicating that the methyl group remains intact on heating to 400°C. These results corroborate the observed chemical analyses, ^{29}Si NMRs, and the DRIFT spectra (see below), all of which indicate that the polymeric character of the material is retained at 400°C.

(B) 600°C

As seen in Fig. 3(a), the species responsible for the −18-ppm peak are no longer present in the 600°C spectrum, although the peak centered at −30 ppm remains. However, the majority of the Si centers now experience a new magnetic environment that results in a peak at ≈−46 ppm. The corresponding CP spectrum (Fig. 3(b)) contains two components at −30 and −45 ppm, with the −30-ppm peak somewhat enhanced by the applied cross-polarization.

The ^{13}C CP NMR (Fig. 4) is quite different from the 400°C spectrum. It now presents very broad peaks typical of amorphous glasses (3000-Hz linewidth) rather than cross-linked polymer. The peak present at 400°C is gone suggesting disappearance of all C–N single bonds, although the Fig. 1 data indicate that the carbon is not lost (see below). Two components are present in the sp^2 and sp^3 regions of the spectrum. The sp^2 C signal is associated with numerous spinning sidebands characteristic of considerable chemical shift anisotropy typical of aromatic hydrocarbon compounds such as pyrene, coronene, and graphite. The sp^3 signal is typical of an amorphous carbon phase as confirmed by Raman spectroscopy, as discussed below.

(C) 800°, 1000°, and 1400°C

Continued heating to 800°, to 1000°, and then to 1400°C diminishes and then eliminates the contribution of the −30-ppm component and shifts the main peak in the ^{29}Si NMR to −49 ppm. At these temperatures, the low H content (Table I) prevents the application of CP for either ^{29}Si or ^{13}C spectra. Indeed, it is no longer possible to obtain meaningful ^{13}C spectra without recourse to very long relaxation times. Note that the 1400°C ^{29}Si spectrum is identical to the 1000° spectrum and is therefore not shown.

(D) NMR Computer Simulation

NMR computer simulation[27,28] of all of the ^{29}Si spectra permits clear-cut identification and quantification of the various silicon species contributing to the individual spectra. Short pulse angles and relatively long recycle delays were chosen to overcome the problem of long ^{29}Si relaxation times and allows the quantitative analysis of the various ^{29}Si environments. The results of the computer simulation studies are presented in Table II. The procedure used was the following. The CP ^{29}Si MAS NMR spectra were simulated to obtain precise chemical shifts. Then, these values were used to simulate the MAS NMR data. Three components appear in the spectra at approximately −18, −30, and −45 ppm. These peaks can be assigned respectively to SiH_2N_2, $SiHN_3$, and SiN_4 units. The assignments of the first two peaks are based on the ^{29}Si chemical shifts found for the 200°C polymer and the corresponding peak intensity changes that occurred during CP. In the 400°C spectrum, the −18 ppm peak is greatly enhanced compared to the −30 ppm peak, indicating more hydrogens per silicon. The assignment of the third peak to SiN_4 sites relies on previously published chemical shift values for crystalline silicon nitride phases (−46.8 and −48.9 ppm for α-Si_3N_4 and −48.7 ppm for β-Si_3N_4).[29–32]

Using these assignments, the following general events are observed to occur. At 400°C, the silicon atoms are in local environments similar to those of the starting polymer with a higher cross-link density that "blurs" the unique magnetic environments about each Si, forcing line broadening. At 600°C, the environment changes drastically, with more than 80% of the Si atoms existing as SiN_4 units. This is primary evidence for the formation of a silicon nitride phase. Given that the 600°C polymer sample is analyzed after a 1-h hold at temperature, it is likely that longer hold times will force the remaining 20% of the Si centers into a SiN_4 magnetic environment, as occurs on incremental heating to 800° or 1000°C.

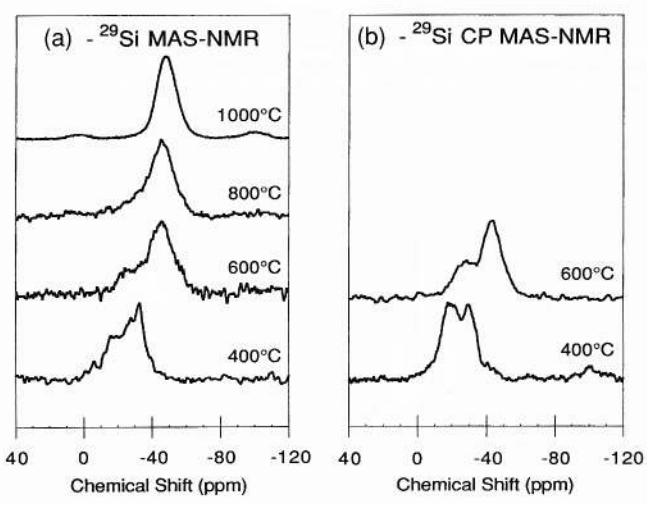

Fig. 3. ^{29}Si MAS (a) and CP-MAS (b) NMR spectra of $-[H_2SiNMe]_x-$ samples pyrolyzed to selected temperatures. Ramp rate of 5°C/min/N_2 followed by a 1-h hold at temperature. The bands around 0 and −100 ppm are spinning side bands.

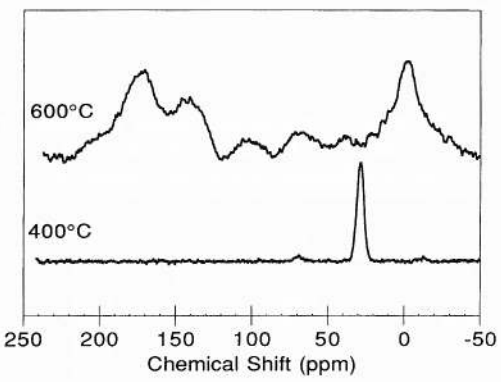

Fig. 4. ^{13}C CP-MAS NMR spectra of $-[H_2SiNMe]_x-$ samples pyrolyzed to 400° and 600°C. Ramp rate of 5°C/min/N_2 followed by a 1-h hold at temperature.

Table II. Results of the Simulation of the ^{29}Si MAS NMR Spectra of the Pyrolyzed Samples

Temperature (°C)	Chemical shift (ppm)	Line width (Hz)	%
400	−31.5	804.5	53.6
	−18.5	1273.5	46.4
600	−45.0	1304.0	83.1
	−30.0	795.0	8.8
	−23.0	715.5	8.1
800	−46.0	1192.5	85.0
	−32.0	795.0	9.6
	−24.0	795.0	5.4
1000	−49.5	1113.0	100.0

At 1000°C, the ^{29}Si MAS NMR can be simulated with a single line centered at −49 ppm with a 1110-Hz line width. The 1400°C spectrum (not shown) is nearly identical to the 1000°C spectrum, although there is some slight line broadening (to 1200 Hz). These values are narrower than those (1600 Hz) previously reported for amorphous silicon nitride.[21–25]

(3) DRIFTS

The DRIFT spectra shown in Fig. 5 were obtained using bulk samples prepared in a manner identical to the MAS NMR samples. At room temperature (rt), the spectrum is characteristic of a polymeric material. The very small peak at 3450 cm^{-1} corresponds to the νN–H of the CH_3NHSiH_2–polymer endcaps. The peaks at 2800–3050 cm^{-1} correspond to the νC–H of the CH_3N– groups. The prominent peak at ≈2090 cm^{-1} corresponds to νSi–H of –SiH_2NMe–. Spectra taken at 1000°C were essentially identical to the 800°C sample and thus are not shown. Spectra taken at 1200° and 1400°C are also nearly identical except for the absence of the small peaks at 2090 and 2850–3050, which disappear as the hydrogen content drops to <0.3 wt%.

(A) 200°C

Incremental heating of the polymer to 200°C causes no apparent changes in the spectrum as would be predicted from the ^{29}Si NMR results, although the νN–H peak is somewhat broader.

(B) 400°C

At this temperature, many of the peaks start to broaden slightly as cross-link density increases; however, the peak positions and their relative intensities all remain approximately equivalent. The νN–H peak appears to increase in intensity and broaden slightly. This may be as a result of some C–N bond cleavage at this temperature (see discussion). These results again correlate with the ^{29}Si and ^{13}C NMR data.

(C) 600°C

As expected, based on the chemical analysis and ^{29}Si NMR results, the 600°C spectrum indicates that the transition to a ceramic has occurred, as evidenced by the appearance of broad peaks for each type of stretching vibration—indicative of a much wider range of physical environments than possible in the polymer. Two key events are the significant decrease in intensities of the νC–H and νSi–H peaks, corroborating the Fig. 1 data. Coincidentally, the 3450-cm^{-1} peak for νN–H has grown in relative intensity. Still other peaks appear in the region of 1480, 1620, and 1730 cm^{-1}. The 1480- and 1620-cm^{-1} peaks are typically associated with aromatic rings such as formed during the graphitization of organic polymers.[33] The peak at 1730 cm^{-1} may be due to νC=N or νC=O absorptions indicating the formation of species containing C–N or C–O double bonds. An alternate interpretation would be that it is an overtone of νN–H at 3450 cm^{-1}.

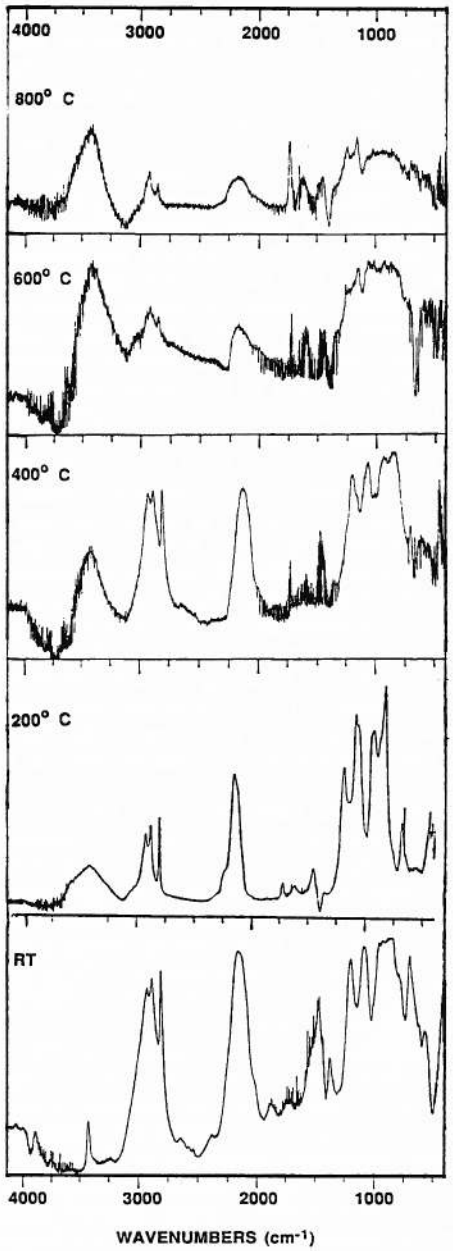

Fig. 5. Diffuse reflectance infrared fourier transform spectra (DRIFTS) of –$[H_2SiNMe]_x$– samples pyrolyzed to selected temperatures. Data points for 1-g samples heated at 5°C/min/N_2 to temperature and held for 1 h.

(D) 800°C

By 800°C, the νC–H and νSi–H peaks are much diminished, and there is a considerable reduction in the νN–H peak. By comparison, the relative intensities of the peaks at approximately 1480, 1620, and 1730 cm^{-1} have grown in intensity and become better resolved. In particular, the peak at 1730–1750 cm^{-1} is now one of the better-resolved peaks in the spectrum. Given that the ^{13}C NMR indicates that most of the carbon at 600°C is present as graphitic or amorphous carbon, it could be argued that the 1730–1750 cm^{-1} is an overtone of the strong νN–H peak rather than a species that incorporates N or O; however, chemical analysis indicates the presence of excess nitrogen and supports the possibility of species containing C=N, which can exhibit stretching absorptions in this region.

III. Discussion

The salient features of the poly(N-methylsilazane) polymer-to-ceramic transformation are readily discernible using ^{29}Si,

^{13}C MAS NMR, and DRIFT spectroscopic techniques and chemical analysis. The first of these is that the precursor polymer undergoes considerable cross-linking (by ^{29}Si NMR and DRIFTS) on heating to 400°C for 1 h, although it does not appear to undergo mineralization.

After 1 h of pyrolysis at 600°C, the ^{29}Si MAS NMR spectrum contains both residual "polymer" peaks (-30 to -35 ppm) and the ceramic product peak (-46 ppm), with the major portion of the material being the ceramic product. These results indicate that the polymer-to-ceramic transition temperature is close to 600°C, and only the hold time at 600°C determines whether the recovered material is polymer or ceramic. Another way of interpreting the results is to say that the kinetics and/or thermodynamics that control the transformation process(es) permit reasonable reaction rates to be reached only at temperatures close to 600°C. This interpretation is supported by all of the analytical techniques used.

It can be argued that the 600°C ^{29}Si MAS NMR signal at -46 ppm is sufficiently close to the peak position reported for amorphous silicon nitride[21–25] as to indicate that phase-pure Si_3N_4 forms at this temperature. However, considerable hydrogen (as N–H bonds by DRIFTS) remains in the material, which contradicts this interpretation. Pyrolysis studies on the conversion of poly(Si-methylsilane) to SiC have shown that elimination of residual hydrogen is necessary to obtain a well-ordered, β-SiC ceramic phase.[34] Ordering is readily observed in the ^{29}Si NMR, as the number of silicon magnetic environments diminishes, leading to significant narrowing of the ^{29}Si peak width. Ordering can occur well before crystallization can be observed by XRD.[34]

In the present case, further heating to 1400°C results in continued loss of hydrogen (Fig. 1, Table I). Coincident with the hydrogen loss, the once-intense νN–H and νC–H bands in the DRIFT spectrum diminish and then disappear and a single, narrow peak at -49 ppm appears in the ^{29}Si MAS NMR. This ^{29}Si peak has a width of only 1100–1200 Hz, which is narrower than that previously reported for amorphous silicon nitride (1600 Hz). The loss of hydrogen coincides with our inability to obtain CP MAS NMR spectra at 800°C.

For comparison purposes, we include the ^{29}Si MAS NMR for $-[MeHSiNH]_x-$ (Fig. 6) produced as in reactions (3) and (4) and heat-treated under conditions identical to those used to obtain the data in Fig. 3. These NMR data clearly illustrate the disorder and exceptional differences in ^{29}Si magnetic environments between the pyrolysis products derived from $-[H_2SiNMe]_x-$ and $-[MeHSiNH]_x-$. More detailed studies on the poly(Si-methylsilazane) pyrolysis studies will be presented at a later date.[14,15]

By 1000°C, only very small amounts of hydrogen remain (0.70 wt%), bound primarily as N–H and some C–H. Given that chemical analysis (at 1000°C) indicates that more nitrogen is present than can be accounted for simply by bonding to silicon, it is quite possible that some of the hydrogen present is bonded to nitrogen, not bound to silicon. At 1400°C, the hydrogen content decreases to 0.28 wt% and the nitrogen content (N/Si ratio = 1.28) is close to that expected (1.33) if all of the silicon is present as silicon nitride.

Three questions remain to be answered: (1) is the amorphous silicon nitride truly amorphous or nanocrystalline, (2) what happened to the carbon, and (3) where is the excess nitrogen seen in the chemical analysis at 1000°C? To determine whether the silicon nitride is truly amorphous or nanocrystalline, samples of the polymer were pyrolyzed to 1000°, 1200°, and 1400°C for 1 h and the resulting powders examined by transmission electron microscopy (TEM) and small-area diffraction (SAD). Neither of these analytical methods provided any indication of crystallinity. The 1400°C sample was examined in more detail by TEM, SAD, Raman spectroscopy, and EELS with the following results.

Figure 7 provides a TEM image with the corresponding SAD diffraction pattern superimposed. The TEM image shows no evidence of crystallinity. The absence of discernible rings in the

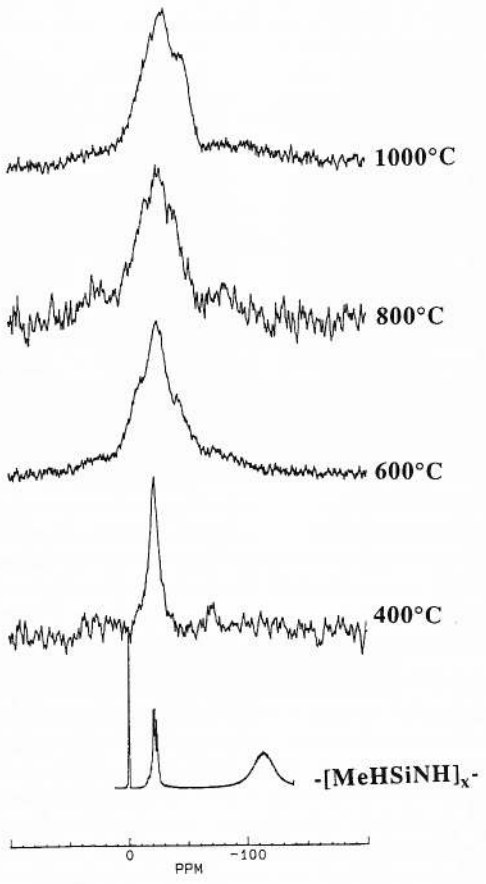

Fig. 6. ^{29}Si MAS NMR spectra of $-[H_2SiNMe]_x-$ samples pyrolyzed to selected temperatures. Ramp rate of 5°C/min/N_2 followed by a 1-h hold at temperature.

circle of illumination for the SAD pattern supports our contention that the sample is amorphous. The portion of the disk seen in the SAD can be attributed to the carbon coating on the grid. Efforts to prepare thin specmens by microtoming particles mounted in a polymer matrix were unsuccessful, as both sapphire and diamond microtome blades were insufficiently sharp/hard enough to provide clean, thin samples.

The TEM studies on the 1400°C sample support the 1000° and 1400°C ^{29}Si MAS NMR results, all of which suggest that any silicon nitride present is amorphous. These findings are also supported by our earlier work, which indicated that only after heating the poly(N-methylsilazane)-derived material to greater than 1600°C for extended periods under 1 atm of N_2 was it possible to see crystalline α- and β-Si_3N_4.[12] It is important to note that no evidence was found for the coincidental formation of SiC.

Amorphous silicon nitride has previously been shown to crystallize readily at ≥1400°C.[8c] Thus, our continued observation of a fully amorphous material at 1400°C is somewhat surprising. One explanation for the stability of the amorphous phase is that the presence of significant amounts of carbon at the individual silicon nitride "grain" boundaries acts as a barrier to diffusion, thereby inhibiting crystallization of silicon nitride. Given the fact that (1) crystallization of amorphous silicon nitride frequently requires the presence of oxygen contaminants,[8c] (2) crystallization is proposed to occur via a VLS mechanism,[35] and (3) minimal amounts of O are present (<1%, detectable to ≈1% by ^{29}Si MAS NMR) in the current composite material, limited potential exists to form glassy phases that can promote diffusion and crystallization. If standard sintering aids (e.g., yttria) are mixed with the polymer before pyrolysis, then it is possible to obtain quite good densification and crystallization with carbon retention.[36]

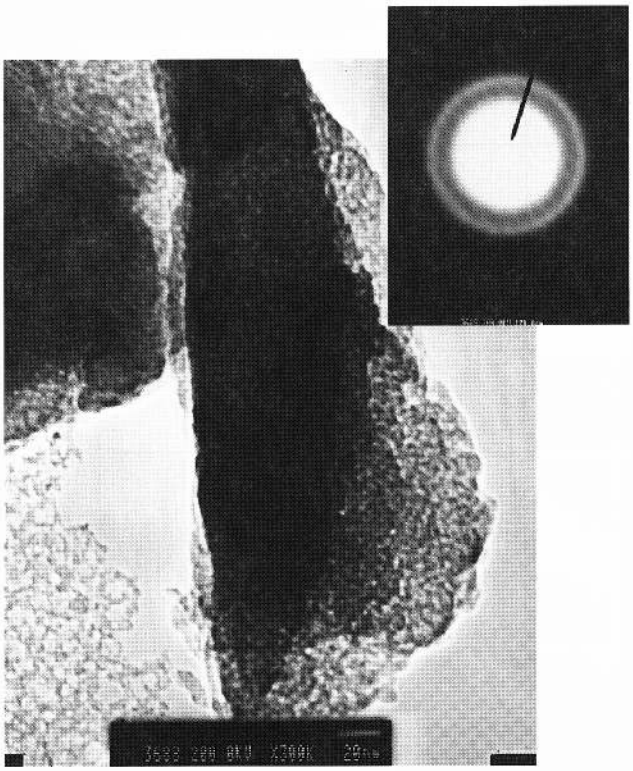

Fig. 7. TEM image with superimposed SAD of 1400°C particles. Both analytical methods indicate that the sample is amorphous.

Efforts to delineate the fate of the carbon "lost" from the N-methyl groups during pyrolysis focused on the use of Raman spectroscopy. Spectra acquired following pyrolysis at 1000°, 1200°, and 1400°C reveal no sharp first-order bands in the regions ascribed to C–H (2900–3100 cm^{-1}) or C≡C (2100–2300 cm^{-1}) stretching vibrations, strongly suggesting the absence of these functional groups in the pyrolyzed materials. A complex band profile is present in the 1300–1600-cm^{-1} region, and weak features near 1100 and 450 cm^{-1} can be seen in the spectrum of the 1400°C pyrolyzed material shown in Fig. 8(a). Spectra acquired from materials pyrolyzed at 1200° and 1000°C are qualitatively similar, but also exhibit a broad fluorescence emission baseline which increases in intensity toward the red end of the spectrum. Fluorescence emission is noticeably reduced in materials pyrolyzed at higher temperatures or when Raman excitation with longer wavelength light is used.

Figure 8(b) shows an expanded trace of the 1100–1800-cm^{-1} region. The complex band contour is fit by three Gaussian components located at 1340, 1533, and 1595 cm^{-1} with line widths of 185, 130, and 74 cm^{-1}, respectively. Band assignments for the modes at 1595 and 1340 are based on a recent publication by Visscher *et al.*,[37] which describes work involving characterization of hard carbon products formed by the pyrolysis of conjugated carbon-containing polymers. The feature at 1595 cm^{-1} is ascribed to microcrystalline graphite. A significantly broader feature (200-cm^{-1} line width) at 1340 cm^{-1} has been assigned to both graphitic carbon and disordered sp^3 bonded carbon due to its proximity to the principal line in diamond at 1333 cm^{-1}. The assignment of the 1340-cm^{-1} feature to a disordered diamond-like carbon is based on previous work involving vapor phase deposition of carbon films.[38,39]

The third mode, located at 1540 cm^{-1}, requires additional explanation. The polymer precursor to the pyrolyzed product contains principally silicon, carbon, nitrogen, and hydrogen. As the polymer decomposes, formation of –C=N– moieties in the structure is likely. The vibrational frequency of such units may be estimated based upon the known frequency of graphitic carbon (1607 cm^{-1})[37] and the ratio of the reduced masses (μ) for –C=C– and –C=N–. Here, $1/\mu_{CN} = 1/12 + 1/14$, and $1/\mu_{CC} = 1/12 + 1/12$. Because the bond-stretching force constant (f) can be written in terms of the vibrational frequency ω and the reduced mass of the oscillator, an estimate of the –C=N– mode frequency becomes possible if the bond force constants are similar:

$$f = \mu\omega^2 \tag{5}$$

$$\omega_{CN} = \omega_{CN}[\mu_{CN}/\mu_{CC}]^{0.5} \tag{6}$$

Therefore, the predicted frequency for the –C=N– mode is 1540 cm^{-1}, in good agreement with the fitted peak at 1533 cm^{-1}. If this analysis is correct, and the 1540-cm^{-1} peak actually corresponds to a –C=N– stretching mode in the 1400°C material, based on our contention that silicon is bound only to nitrogen in this material, we must conclude that this silicon nitride is in the form of highly dispersed particles bounded by carbon and frequently bound to carbon. In essence, if our assessment is correct, the Raman data provide a spectroscopic view of the silicon nitride–carbon interface at the atomic level.

Finally, the weak feature at 1100 cm^{-1} with a line width of ≈400 cm^{-1}, is assigned to sp^3 hybridized carbon in a highly disordered environment.[37] Based on these assignments, the pyrolyzed product contains significant percentages of disordered carbon present in both sp^2 and sp^3 bonding environments. The weak, low-frequency mode near 460 cm^{-1} and the breadth of the 1100-cm^{-1} mode are indicative of amorphous Si_3N_4 as described by Wada *et al.*[40] Raman measurements, therefore, confirm the presence of both graphitic and diamond-like carbon regions in an amorphous silicon nitride matrix and suggest the presence of –C=N– moieties at the interface. These carbon analyses are qualitatively consistent with the ^{13}C CP MAS NMR data at 600°C, the highest temperature at which ^{13}C MAS NMRs could be realistically obtained.

The final question of where the excess nitrogen is located in the 1000°C ceramic product still remains unresolved. The DRIFT spectra at 800°C show a peak at 1730–1750 cm^{-1} that could simply be an overtone of the very strong νN–H peak at 3450 cm^{-1} or result from the presence of species containing C=N and/or C=O bonds. If we consider that on heating from 600° to 800°C the νN–H at 3450 cm^{-1} diminishes in intensity relative to the band at 1730–1750 cm^{-1}, we can argue that the two bands are not coupled harmonically. Consequently, we can argue for the presence of C=N and/or C=O bonds in the product. Given the excess nitrogen and the Raman results for the higher temperature materials, we believe that it resides in moieties that contain C=N bonds and thus we are seeing a νC=N peak. This is not unexpected, given that previous efforts to make carbon nitride typically fail because of the evolution of cyanide-containing species.[41,42] A species containing C=N is well on its way to forming cyanide containing leaving groups (e.g., HC≡N or N≡C–C≡N). The loss of these types of species would account for the somewhat lower carbon and nitrogen contents at 1400°C.

IV. Conclusions

The analytical data from the DRIFTS, ^{13}C and ^{29}Si MAS and CP MAS NMR, and chemical and Raman analysis indicate that the product derived from pyrolysis of poly(N-methylsilazane) is a composite of nearly phase-pure (very narrow ^{29}Si NMR line width) amorphous silicon nitride particles bounded by a mixed graphitic/amorphous carbon phase. The evidence against the presence of Si–C bonds is all negative in that none are observed by NMR or DRIFTS or suggested by the analytical data. Efforts to identify crystalline phass by TEM for samples heated to 1400°C were unsuccessful, indicating that the product remains amorphous.

The fact that the $-[H_2SiNMe]_x-$ derived material remains amorphous at temperatures where other researchers observe ready crystallization of amorphous silicon nitride,[8c] but with

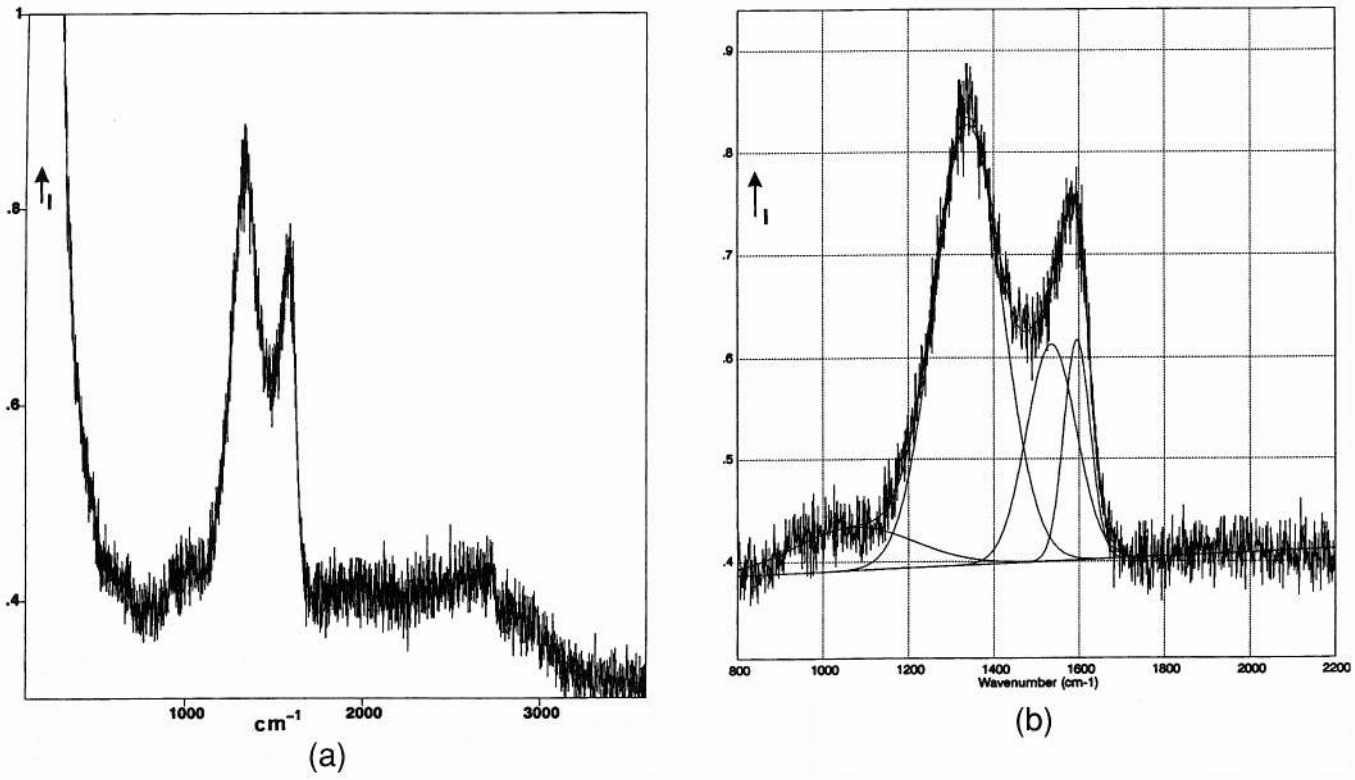

Fig. 8. (a) Raman spectrum of $-[H_2SiNMe]_x-$ pyrolyzed to 1400°C. Data points for 1-g samples heated at 5°C/min/N_2 to temperature and held for 1 h. (b) Best-fit Gaussian peaks to the band contour in the carbon–carbon stretching region.

samples containing significant amounts of oxygen, suggests that oxygen-containing species (e.g., SiO and SiO_xN_y) play an important role in the proposed VLS crystallization mechanism.[35] This conclusion is supported by the facile crystallization of $-[H_2SiNMe]_x-$ derived material in the presence of common sintering aids (e.g., Y_2O_3), which aid crystallization through formation of glassy oxynitride phases.[36] An alternate interpretation is that there is no facile mechanism for diffusion at the amorphous silicon nitride particle–carbon interface, and thus grain growth and crystallization are prevented.

Finally, it is important to note that the results reported above clearly indicate that the architecture of the monomer unit in a preceramic polymer can have a significant impact on selectivity to ceramic product(s) and perhaps the evolution (or lack thereof) of the microstructure.

Acknowledgments: RML and FB would like to thank Dr. Corine Gérardin (Chime de la Matière Condensée, Université Pierre et Marie Curie) Paris, France for very fruitful discussions concerning the NMR of polysilazanes. Dr. Dominique Massiot (CRPHT, CNRS, Orléans, France) is also gratefully acknowledged for the NMR simulation programs. The authors would also like to thank Dr. Cathy Scotto for synthesis of samples of $-[H_2SiNMe]_x-$ at the University of Michigan, and Dr. Zhi-Fan Zhang for demonstrating the reproducibility of the DRIFTS studies.

References

[1](a) D. Seyferth and G. H. Wiseman, "Silazane Precursors to Silicon Nitride"; pp. 265–71 in *Ultrastructure Processing of Ceramics and Composites*. Edited by L. L. Hench and D. R. Ulrich. Wiley, New York, 1984. (b) D. Seyferth, "Organosilicon Polymers as Precursors for Silicon-Containing Ceramics"; pp.133–54 in *Transformation of Organometallics into Common and Exotic Materials: Design and Activation*, NATO ASI Ser. E: Appl. Sci. No. **141**. Edited by R. M. Laine. Kluwer, Dordrecht, Netherlands, 1988, and references therein.

[2]B. G. Penn, F. E. Ledbetter III, and J. M. Clemons, "An Improved Process for Preparing *tris*(N-methylamino)methylsilane Monomer for Use in Producing Silicon Carbide–Silicon Nitride Fibers," *Ind. Eng. Chem. Process Des. Dev.*, **23**, 217–20 (1984) and references therein.

[3]N. S. C. K. Yive, R. J. P. Corriu, D. Leclercq, P. H. Mutin, and A. Vioux, "Thermogravimetric Analysis/Mass Spectrometry Investigation of the Thermal Conversion of Organosilicon Precursors into Ceramics under Argon and Ammonia. 2. Poly(silazanes)," *Chem. Mater.*, **4**, 1263–71 (1992).

[4](a) R. Baney and G. Chandra, "Preceramic Polymers," *Encycl. Polym. Sci. Eng.*, **13**, 312–44 (1988). (b) R. R. Wills, R. A. Markle, and S. P. Mukherjee, "Siloxanes, Silanes, and Silazanes in the Preparation of Ceramics and Glasses," *Am. Ceram. Soc. Bull.*, **62**, 904–15 (1983).

[5]G. T. Burns, T. P. Angelotti, L. F. Hanneman, G. Chandra, and J. A. Moore, "Alkyl- and Arylsilsesquiazanes: Effect of the R Group on Polymer Degradation and Ceramic Char Composition," *J. Mater. Sci.*, **22**, 2609–14 (1987).

[6]Y. Nakaido, Y. Otani, N. Kozakai, and S. Otani, "Silicon Nitride Carbide Fibers from Spinnable Polymethylsilazanes," *Chem. Lett.*, 705–706 (1987).

[7]F. Siriex, P. Goursat, A. Lecomte, and A. Dauger, "Pyrolysis of Polysilazanes: Relationship between Precursor Architecture and Ceramic Microstructure," *Compos. Sci. Technol.*, **37**, 7–19 (1990).

[8](a) T. Vaahs, Hoechst Data Sheet, "Ceramics from Polymers, Polysilazane VT 50," 1990. (b) R. Riedel, M. Seher, and G. Becker, "Sintering of Amorphous Polymer-Derived Si, N and C Containing Composite Powders," *J. Eur. Ceram. Soc.*, **5**, 113–22 (1989). (c) R. Riedel and M. Seher, "Crystallization Behaviour of Amorphous Silicon Nitride," *J. Eur. Ceram. Soc.*, **7**, 21–25 (1991).

[9](a) N. S. C. K. Yive, R. J. P. Corriu, D. Leclercq, P. H. Mutin, and A. Voiux, "Silicon Carbonitride from Polymeric Precursors: Thermal Cross-linking and Pyrolysis of Oligosilazane Model Compounds," *Chem. Mater.*, **4**, 141–46 (1992). (b) N. S. C. K. Yive, R. Corriu, D. Leclercq, P. H. Mutin, and A. Voiux, "Polyvinylsilazane: A Novel Precursor to Silicon Carbonitride," *New J. Chem.*, **15**, 85–92 (1991).

[10]K. A. Youngdahl, R. M. Laine, R. A. Kennish, T. R. Cronin, and G. A. Balavoine, "New Catalytic Routes to Preceramic Polymers: Ceramic Precursors to Silicon Nitride and Silicon–Carbide Nitride," *Mater. Res. Symp. Symp. Proc.*, **121**, 489–95 (1988).

[11]R. M. Laine, "Transition Metal Catalyzed Synthesis of Oligo- and Polysilazanes and Their Use as Precursors to Silicon Nitride Containing Ceramic Materials," *Platinum Met. Rev.*, **32**, 64–71 (1988).

[12]Y. D. Blum, K. B. Schwartz, and R. M. Laine, "Preceramic Polymer Pyrolysis. I. Pyrolytic Properties of Polysilazanes," *J. Mater. Sci.*, **24**, 1707–17 (1989).

[13]R. M. Laine, Y. Blum, D. Tse, and R. Glaser, "Synthetic Routes to Oligo- and Polysilazanes. Polysilazane Precursors to Silicon Nitride"; pp. 124–42 in *Inorganic and Organometallic Polymers*. Edited by K. Wynne, M. Zeldin, and H. Allcock. American Chemical Society, Washington, DC, 1988.

[14]R. M. Laine, F. Babonneau, J. A. Rahn, Z.-F. Zhang, and K. A. Youngdahl, "The Effect of Monomer Architecture on Selectivity to Ceramic Products and Microstructure in Silicon Preceramic Polymers"; pp. 159–69 in Thirty-Seventh Sagamore Army Materials Research Conference Proceedings. Edited by D. J. Viechnicki. Publications Department of the Army, 1991.

[15]F. Babonneau, K. A. Youngdahl, J. A. Rahn, C. Scotto, and R. M. Laine, unpublished work—see Ref. 14 for some preliminary results.

[16]G. E. Legrow, T. F. Lim, J. Lipowitz, and R. S. Reaoch, "Ceramics from Hydridopolysilazane," *Am. Ceram. Soc. Bull.*, **66**, 363–67 (1987).

[17](a) J. Lipowitz, H. A. Freeman, R. T. Chen, and E. R. Prack, "Composition and Structure of Ceramic Fibers Prepared from Polymer Precursors," *Adv.*

Ceram. Mater., **2**, 121–28 (1987). (b) J. Lipowitz, J. A. Rabe, and T. M. Carr, "Characterization of the Reaction Products of Symmetrical Dimethyltetrachlorodisilazane with Hexamethyldisilazane by ^{29}Si NMR Spectroscopy," *Spectrosc. Lett.*, **20**, 53–65 (1987).

[18]R. H. Lewis, R. A. Wind, and G. E. Maciel, "Investigation of Cured Hydridopolysilazane-Derived Ceramic Fibers via Dynamic Nuclear Polarization," *J. Mater. Res.*, **8**, 649–54 (1993).

[19]T. Taki, M. Inui, K. Okamura, and M. Sato, "A Study of the Nitridation Process of Polycarbosilane by Solid-State High-Resolution NMR," *J. Mater. Sci. Lett.*, **8**, 1119–21 (1989).

[20]Y. H. Mariam and P. Abrahams, "2D Heteronuclear Chemical Shift Correlated Spectroscopy of Carbosilyl Amine Polymers," *Polym. Prepr. (Am. Chem. Soc. Div. Polym. Chem.)*, **29**, 364 (1988).

[21]G. T. Burns and G. Chandra, "Pyrolysis of Preceramic Polymers in Ammonia: Preparation of Silicon Nitride Powders," *J. Am. Ceram. Soc.*, **72**, 333–37 (1989).

[22]T. Isoda, "Surface of High Purity Silicon Nitride Fiber Made from Perhydropolysilazane"; pp. 255–65 in *The Third International Conference on Composite Interfaces (ICCI-III): Controlled Interface Structures*. Edited by H. Ishida. Elsevier, New York, 1990.

[23]Y. Yokoyama, T. Nanba, I. Yasui, H. Kaya, T. Maeshima, and T. Isoda, "X-ray Diffraction Study of the Structure of Silicon Nitride Fiber Made from Perhydropolysilazane," *J. Am. Ceram. Soc.*, **74**, 654–57 (1991).

[24]H. Aoki, T. Suzuki, T. Katahata, M. Haino, G. Nishimura, H. Kaya, T. Isoda, Y. Tashiro, O. Funayama, and M. Arai, "Silicon Nitride Based Ceramic Fibers, Process of Preparing Same and Composite Materials Containing Same," Eur. Pat. Appl. 0 332 357, March, 1989.

[25]S. Schaible, R. Riedel, E. Werner, and U. Klingebiel, "From Cyclotetrasilazane $[(CH_3)_2SiNH]_4$ via Crystalline Silicon Nitride Imide Si_2N_2NH to α-Si_3N_4," *Appl. Organomet. Chem.*, **7**, 53–56 (1993).

[26]T. M. Duncan, *A Compilation of ^{29}Si Chemical Shift Anisotropies*. The Farragut Press, Chicago (1990).

[27]Simulation programs (FIT) were developed by Dominique Massiot (CRHPT, CNRS, Orléans, France). Ref. 28 provides an example of the application of this technique.

[28]R. M. Laine, K. A. Youngdahl, F. Babonneau, J. F. Harrod, M. L. Hoppe, and J. A. Rahn, "Synthesis and High Temperature Chemistry of Methylsilsesquioxane Polymers Produced by Titanium Catalyzed Redistribution of Methylhydridooligo- and Polysiloxanes," *Chem. Mater.*, **2**, 464–72 (1990).

[29]K. R. Carduner, C. S. Blackwell, W. B. Hammond, F. Reidinger, and G. R. Hatfield, "^{29}Si NMR Characterization of α and β Silicon Nitride," *J. Am. Chem. Soc.*, **112**, 4676–79 (1990).

[30]K. R. Carduner, R. O. Carter III, M. E. Milberg, and G. M. Crosbie, "Determination of Phase Composition of Silicon Nitride Powders by Silicon-29 Magic Angle Spinning Nuclear Magnetic Resonance Spectroscopy," *Anal. Chem.*, **59**, 2794 (1987).

[31]E. A. Williams, "Recent Advances in Silicon-29 NMR Spectroscopy," *Annu. Rep. NMR Spectrosc.*, **15**, 235 (1983).

[32]R. K. Harris, M. J. Leach, and D. P. Thompson, "Synthesis and Magic-Angle Spinning Nuclear Magnetic Resonance of ^{15}N-Enriched Silicon Nitrides," *Chem. Mater.*, **2**, 320–23 (1990).

[33]Y. Wang, D. C. Alsmeyer, and R. L. McCreery, "Raman Spectroscopy of Carbon Materials: Structural Basis of Observed Spectra," *Chem. Mater.*, **2**, 557–63 (1990) and references therein.

[34](a) Z.-F. Zhang, F. Babonneau, R. M. Laine, Y. Mu, J. F. Harrod, and J. A. Rahn, "Poly(methylsilane)—A High Ceramic Yield Precursor to Silicon Carbide," *J. Am. Ceram. Soc.*, **74**, 670–73 (1991). (b) R. M. Laine and F. Babonneau, "Preceramic Polymer Routes to SiC," *Chem. Mater.*, **5**, 260–79 (1993).

[35]T. Yamada, T. Kawahito, and T. Iwai, "Crystallization of Amorphous Si_3N_4 Prepared by the Thermal Decomposition of $Si(NH)_2$," *J. Mater. Sci. Lett.*, **2**, 275–78 (1983).

[36]K. B. Schwartz, D. J. Rowcliffe, and Y. D. Blum, "Microstructural Development in Si_3N_4/Polysilane Bodies during Heating," *Adv. Ceram. Mater.*, **3**, 320–23 (1988).

[37]G. T. Visscher, D. C. Nesting, J. V. Badding, and P. A. Bianconi, "Poly(Phenylcarbyne): A Polymer Precursor to Diamond-Like Carbon," *Science*, **260**, 1496–99 (1993).

[38]J. M. Mendez, S. Muhl, G. Contreras-Puente, and J. Aguilar-Hernandez, "Optical Properties of Amorphous Carbon Thin Films Prepared by Plasma Deposition in a Graphite Hollow Cathode," *Thin Solid Films*, **220**, 125–31 (1992).

[39]C.-F. Chen and T.-M. Hong, "Characterization and Morphological Features of Diamond Films and Particles Affected by a Diamond-Like Pre-Coated Layer," *Surf. Coat. Technol.*, **54/55**, 368–73 (1992).

[40]N. Wada, S. A. Solin, J. Wong, and S. Prochazka, "Raman and IR Absorption Spectroscopic Studies on α, β and Amorphous Si_3N_4," *J. Non-Cryst. Solids*, **43**, 7–15 (1981).

[41]L. Maya and L. A. Harris, "Pyrolytic Deposition of Carbon Films Containing Nitrogen and/or Boron," *J. Am. Ceram. Soc.*, **73**, 1912–16 (1990) and references therein.

[42]M. R. Wixom, "Chemical Preparation and Shock Wave Compression of Carbon Nitride Precursors," *J. Am. Ceram. Soc.*, **73**, 1973–78 (1990) and references therein. □